RICHARD W. CHRISTENSEN, Dames and Moore, Chicago
BRAJA M. DAS, Walter Lum Assoc., Honolulu

HYDRAULIC EROSION OF REMOLDED COHESIVE SOILS

This study was undertaken to gain a better understanding of the erosion of cohesive soils and to determine the relationship between rate of erosion under steady flow conditions and critical tractive stress. Tests were conducted on soils containing kaolinite and grundite, and Ottawa sand was used as an additive in some of the samples. Three series of tests were conducted to determine the effects of test duration and tractive stress, density and moisture content, and temperature of water flow on hydraulic erosion. The first series revealed that there are three distinct stages of erosion under a given tractive stress. In series II, the samples were prepared at varying densities and moisture contents. Molding the samples at high moisture contents produced smoother samples; thus, it appeared that decreasing surface roughness was more important than increasing density. When the temperature of the water flow was varied in series III, it was observed that the rate of erosion increased significantly with increasing temperature. It was concluded that erosion rates are dependent on soil composition, surface roughness, flow rate, temperature, and duration of flow.

In recent years increasing emphasis has been placed on the study of erosion characteristics of cohesive soils. Knowledge of the rate of erosion is especially useful in the design of noneroding canals and maintenance of highway embankments and other man-made structures.

Erosion of cohesive soils under steady flow conditions has been considered for this study. The resistance to erosion of cohesive soils is generally attributed to the interparticle forces and the electrochemical forces between the clay particles. The rate of erosion is a function of the hydraulic tractive stress that causes erosion, of temperature of the flowing water, and of several other soils parameters such as density, moisture content, clay type, percentage of clay fraction, and cation concentration.

An improved understanding of the effects of these parameters has been developed by several researchers (2, 3, 4, 12, 14, 15, 16, 17, 18). However, definite relationships between rates of erosion under steady flow conditions and critical tractive stress are still lacking. This study was conducted for the purpose of supplementing the understanding of erosion processes in cohesive soils.

EXPERIMENTAL STUDIES

Materials

Tests reported in this study were conducted on soils containing kaolinite and grundite as basic clay minerals. Ottawa sand was used as an additive to the clay minerals in some of the soil samples. A description of the soils tested is given in Table 1. All samples were tested in the saturated condition.

Testing Apparatus

A majority of the studies on erosion of cohesive soils in the past have been done by the use of the shear flume. The experimental procedure adopted in this study involves lining the inside of a brass tube (1-in. inside diameter, 4 in. long) with the clay to be tested and maintaining a steady flow of water through the clay linings. The thickness of the clay linings was kept at $\frac{1}{8}$ in. for all the tests conducted.

A schematic diagram of the laboratory experimental setup is shown in Figure 1. Desired rates of flow through the clay linings were maintained by an overhead tank and two flow adjusters. The pipes leading from the overhead tank into and out of the clay-lined brass tube were kept at the same inside diameter as the clay lining ($\frac{3}{4}$ in.) to avoid turbulence.

Sample Preparation

The assembly for lining the inside of the brass tube with clay is shown in Figure 2. It consists of an outer brass tube having an inside diameter of 1 in. (sample tube), an inner molding tube ($\frac{3}{4}$-in. outside diameter) with a socket head at the top and semicircular openings at the bottom, two end pieces, and a plunger.

The clay samples were molded by placing the assembly under a static compression device with the plunger inside the socket head of the inner tube (Fig. 3). When pressure is applied to the plunger, the clay is pushed in and forced through the semicircular holes at the bottom of the inner tube into the $\frac{1}{8}$-in. thick annular space between the inner and outer molding tubes. The plunger is removed and more clay is added into the socket head as required. This process is continued until threads of clay begin to emerge from the small hole in the side of the outer tube. If the emerging threads are observed, the presence of any voids can be detected. After compaction is complete, the plunger is removed, the inner tube is slipped out, and the end pieces are removed. This process produces a smooth clay lining $\frac{1}{8}$ in. thick with a $\frac{3}{4}$-in. inside diameter and 4-in. length on the inside of the outer brass tube.

Samples prepared in this manner proved to be very consistent and reproducible. It is expected that the orientation of clay particles would remain practically the same for samples made from the same type of clay at the same moisture content. After visual examination, disturbed samples were rejected, inasmuch as rough linings would affect the test results.

The weight of the outer brass tube was recorded before the start of the molding procedure and again after the tube was lined with clay. The difference in these two weights gives the weight of the clay used in the lining. If the moisture content during molding is known, the dry weight of the clay can be determined.

Hydraulic Tractive Stress

With a steady rate of flow of water through the sample tube, the hydraulic tractive stress on the surface of the clay lining can be expressed as

$$\tau_H = \frac{f\rho}{8} V^2 \qquad (1)$$

where

τ_H = hydraulic tractive stress on the surface of the clay lining,
f = friction factor for the surface of the clay lining,
ρ = density of water, and
V = average velocity of flow through the clay lining.

The friction factor f in Eq. 1 was evaluated by the use of the Moody diagram (11) as a function of Reynolds number and relative roughness of the material, ϵ/D, where ϵ is a measure of the size of the roughness projection for the surface of the clay lining and D is the inside diameter of the clay lining.

Because the kaolinite and grundite soils used for this study are more than 95 percent finer than 0.045 mm and the innner molding tube used for surface

Table 1. Description of soils tested.

Soil	<No. 40 Sieve (percent)	<No. 200 Sieve (percent)	<2 Microns (percent)	Liquid Limit	Plastic Limit	Plasticity Index
Kaolinite	100	100	53	43	29	14
Grundite	100	96	62	51	30	21
Ottawa sand	2	—	—	—	—	—

Figure 1. Schematic diagram of laboratory erosion test setup.

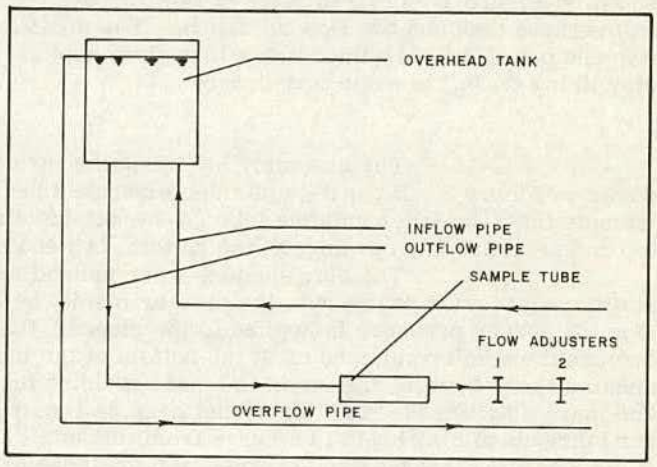

Figure 2. Assembly for clay lining inside brass tube.

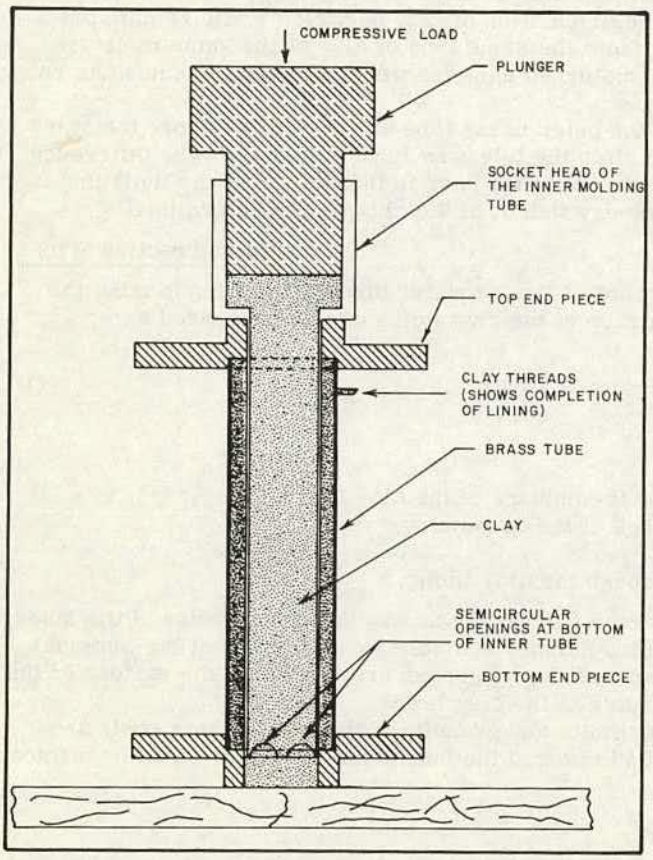

Figure 3. Compaction process for clay lining inside brass tube.

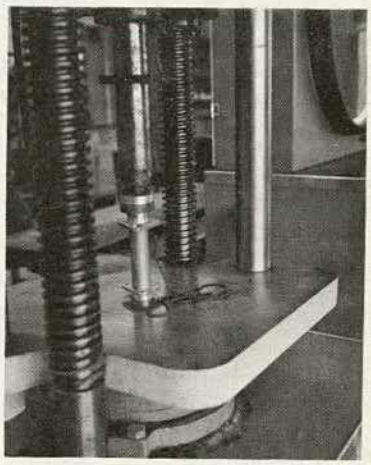

finishing was drawn brass tubing, the inside surface of the clay lining is expected to be very smooth. Hence, the value of ϵ for the clay samples can be expected to be within the range of wrought iron and drawn tubing.

The rate of flow during all the tests was adjusted in such a manner that the Reynolds number remained in the range of 4,000 to 8,000.

Table 2 gives the range of friction factors for wrought iron and drawn tubing for a $\frac{3}{4}$-in. inside diameter at Reynolds numbers of 4,000 and 8,000. It can be seen from Table 2 that, for the given diameter and with the range of Reynolds number between 4,000 and 8,000, the maximum difference in friction factor between wrought iron tubing and drawn tubing is about 12 percent. It may be noted that the friction factor versus Reynolds number plot for the drawn tubing approaches that of smooth pipe flow within the range of Reynolds numbers considered.

The original surface of the clay lining prior to testing should be no rougher than that of wrought iron. During testing, after large amounts of erosion have taken place, the surface tends to become quite rough. However, the test data were disregarded when erosion became excessive. Therefore, if the hydraulic shear stress is computed on the assumption of smooth pipe flow, the results will not be in error by more than 12 percent at the maximum and about 5 to 6 percent on the average. The equation relating Reynolds number and the friction factor for smooth pipe flow may be expressed in the form

$$\frac{1}{\sqrt{f}} = 2 \log_{10} R \times \sqrt{f} - 0.8 \qquad (2)$$

where R = Reynolds number.

Equations 1 and 2 were used for calculation of hydraulic tractive stress on the surface of the clay linings.

Controlled Variables

The effect of three major variables that influence the rate of erosion of cohesive soils, i.e., hydraulic tractive stress on the clay lining, molding moisture content, and temperature of flowing water, have been studied for the two types of clay described. In each series of tests, one of the variables was changed while the others were kept constant. The sequence of laboratory testing is given in Table 3.

TEST RESULTS

Series I

This phase of the investigation was designed to study the erosion of the soil samples for various test durations and hydraulic tractive stresses. The durations of the tests for kaolinite samples were $\frac{1}{4}$, $\frac{1}{2}$, $\frac{3}{4}$, and 1 hour, and those for the grundite samples were $\frac{1}{2}$, 1, 2, and 3 hours. The hydraulic tractive stress was varied by changing the flow rate. The molding moisture content, density, and the test temperature were kept constant for each soil under consideration. The amount of erosion under varying test conditions is shown in Figures 4 and 5.

It can be seen from these figures that, for each soil, there are three distinct stages of erosion under a given hydraulic tractive stress. These three stages are more distinguishable in the case of grundite than kaolinite. In the initial stage, the rate of erosion decreased with time, followed by what appears to be a steady-state condition during which the rate of erosion remained constant. At the end of the steady state, the rate of erosion increased rapidly. During the latter stage, the eroded soil particles were much larger, indicating a rapid deterioration of the clay surface. The shapes of the curves shown in Figures 4 and 5 suggest that, in the early stages of the tests, loose particles left on the surface are eroded away first, followed by a steady-state condition of fairly short duration; and finally, after the surface has been significantly roughened by the previous erosion, the rate of erosion accelerates rapidly, and the surface deteriorates badly in a short period of time. The entire process bears a

Table 2. Friction factors for wrought iron and drawn tubing.

Material	ϵ (ft)	Reynolds Number	D (ft)	ϵ/D	f	Difference (percent)
Wrought iron	0.00015	8,000	1/16	0.0024	0.036	11.7
Drawn tubing	0.000005	8,000	1/16	0.00008	0.0324	
Wrought iron	0.00015	4,000	1/16	0.0024	0.042	5.0
Drawn tubing	0.000005	4,000	1/16	0.00008	0.040	

Table 3. Parameters of the three test series.

Series	Variable Parameters	Controlled Parameters
I	Hydraulic tractive stress on clay lining, duration of test	Density of compaction, molding moisture content, temperature of water
II	Molding moisture content	Hydraulic tractive stress on clay lining, duration of test, temperature of water
III	Temperature of water	Hydraulic tractive stress on clay lining, duration of test, molding moisture content

Figure 4. Erosion versus time at constant temperature and moisture content for kaolinite.

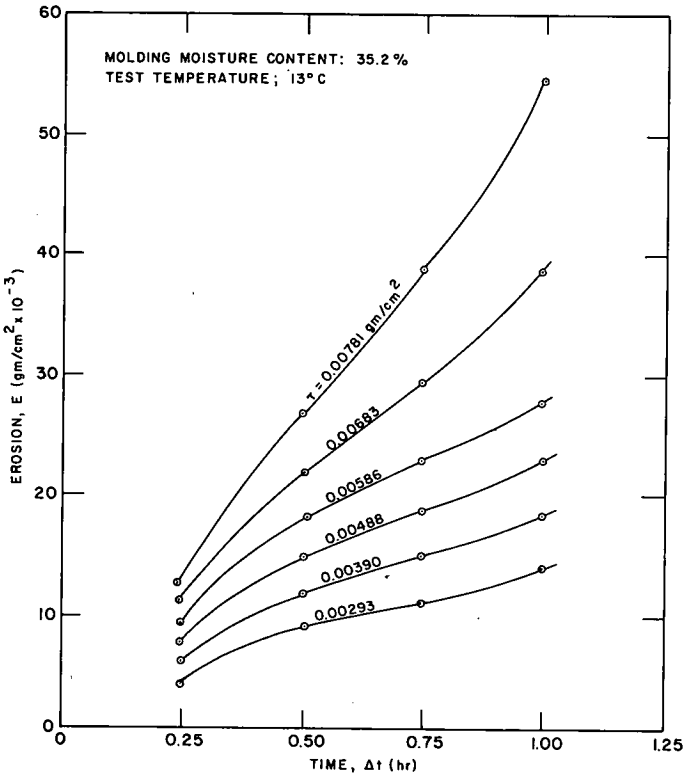

marked resemblance to creep behavior of cohesive soils at stress levels large enough to eventually cause failure.

Figures 6 and 7 show the steady-state rate of erosion as a function of the hydraulic tractive stress for kaolinite and grundite. These curves demonstrate that the steady-state rate of erosion rapidly increased beyond a certain hydraulic tractive stress level for each soil. This point seems to delineate the onset of mass erosion from the surface. The corresponding stress level is termed the "critical" hydraulic tractive stress τ_{cr}. Stress levels higher than τ_{cr} lead to severe erosion of the clay surface in a very short period of time.

Series II

It is generally assumed that, under similar conditions, the rate of erosion will decrease with increasing density. However, the evidence in previous studies has not been conclusive (4, 17, 18).

For this phase of the laboratory investigation, saturated soil samples were prepared at varying densities and moisture contents and subjected to a constant hydraulic tractive stress. Because the soil samples were saturated, the density decreases with increasing moisture content. The duration of the test and the temperature of the water were kept constant for each type of soil.

The laboratory test results, shown in Figures 8 and 9, exhibit a sharp decrease in erosion with increasing moisture content. Visual observation of the samples prior to testing indicated that molding the samples at higher moisture contents produced a smoother surface on the clay lining. It was also observed that the linings containing sand were rougher than those without sand at the same moisture content. From the results obtained in this series of tests, it appears that decreasing the surface roughness is more important than increasing the density from the standpoint of reducing erosion.

Series III

Grissinger (4) has reported that erosion rates are influenced by temperature. In this series of tests, erosion of kaolinite and grundite samples was observed with the flowing water adjusted to various temperatures. Because the clay linings were only $\frac{1}{8}$ in. thick, it is assumed that the temperature of the clay quickly adjusted to the temperature of the flowing water. The configuration of the testing apparatus did not allow direct temperature readings in the clay; therefore, it is not definitely known whether the temperature of the clay completely adjusted to the temperature of the flowing water within the duration of the tests. During this series of tests the molding moisture content, hydraulic tractive stress, and test duration were held constant.

The effects of varying water temperature are shown in Figures 10 and 11. It may be observed that the rate of erosion increased significantly with increasing temperature and that the erosional response to temperature changes is typical of thermally activated processes. It should be noted that the data shown in Figures 10 and 11 may be somewhat in error due to the possibility that the temperature in the clay may not have reached complete equilibrium with the temperature of the flowing water during the time the tests were in progress. Correction of the temperature data, if any is required, would result in a steepening of the slopes of the lines shown in Figures 10 and 11; i.e., a more pronounced temperature effect than that shown.

INTERPRETATION OF RESULTS

The test results obtained in this study bear a striking similarity to those obtained from creep tests on saturated cohesive soils under constant shear stress. Therefore, it may be postulated that, although direct proof would be difficult, particles or clusters of particles are eroded from a clay surface as a result of shear stress transmitted by the flowing water. If so, it should be possible to interpret the erosion behavior of cohesive soils within the same framework as that used to explain steady-state creep behavior.

Figure 5. Erosion versus time at constant temperature and moisture content for grundite.

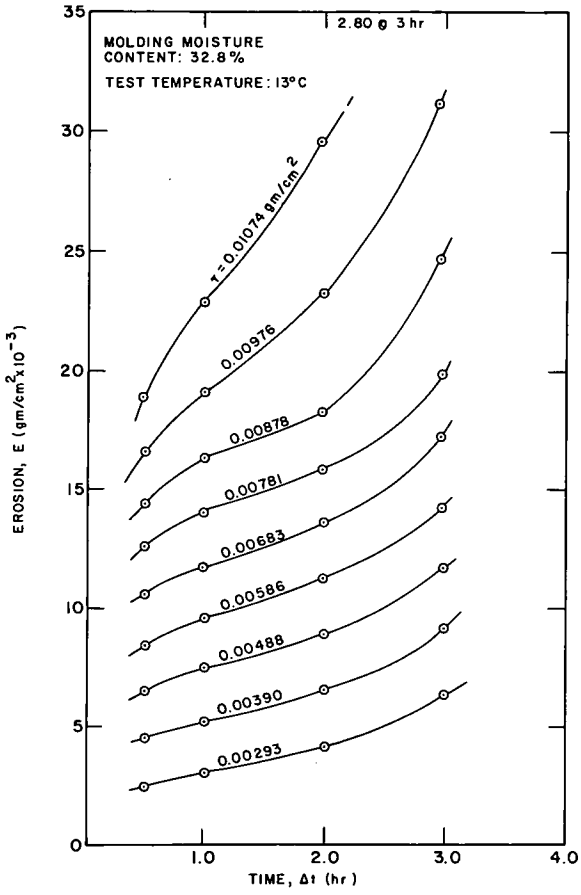

Figure 6. Log E versus hydraulic shear stress at constant temperature and moisture content for kaolinite.

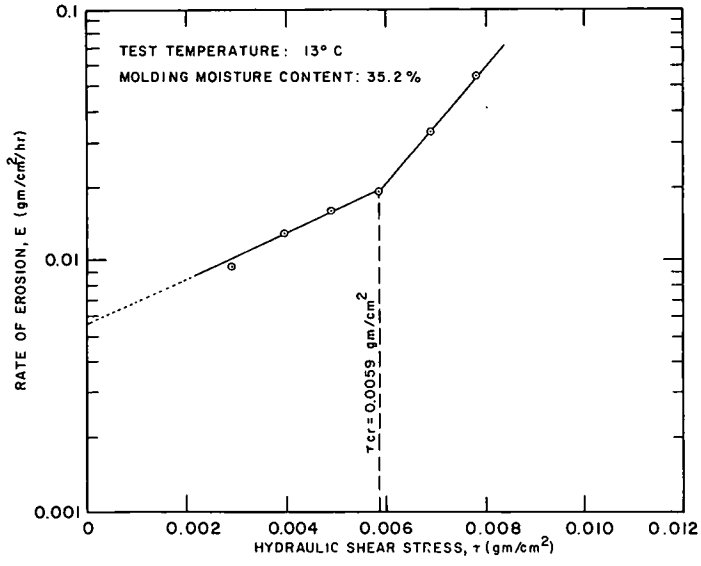

Figure 7. Log E versus hydraulic shear stress at constant temperature and moisture content for grundite.

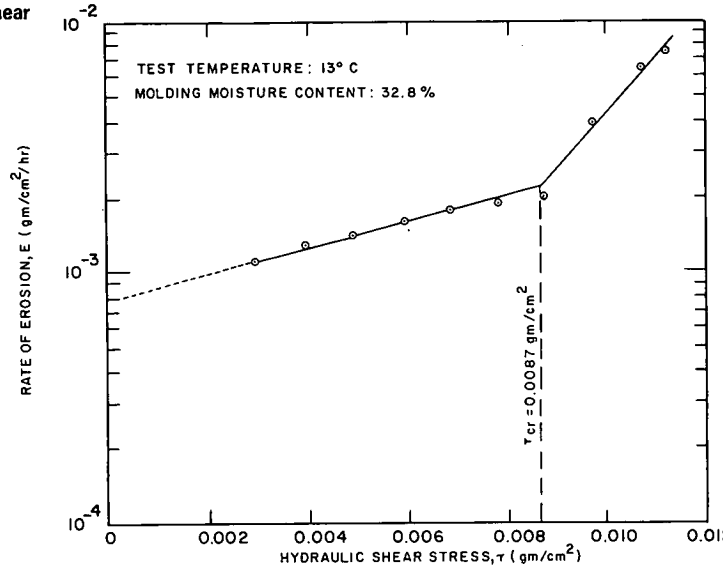

Figure 8. Erosion and dry density versus moisture content at constant temperature and hydraulic shear stress for kaolinite and kaolinite-sand mix.

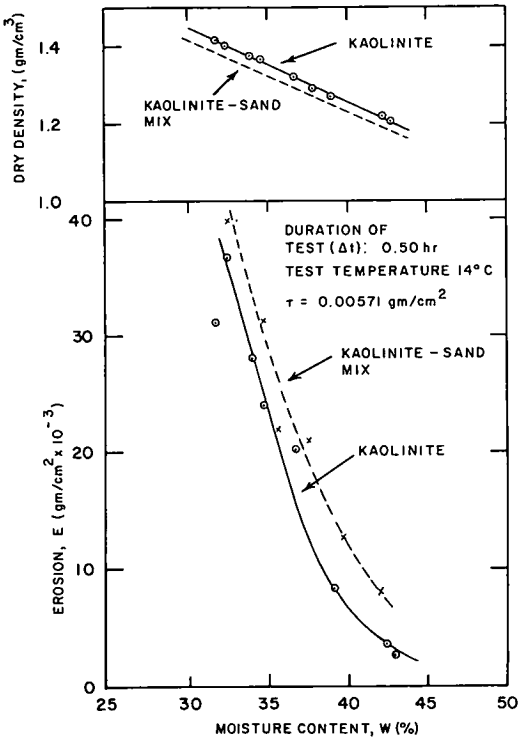

Figure 9. Erosion and dry density versus moisture content at constant temperature and hydraulic shear stress for grundite and grundite-sand mix.

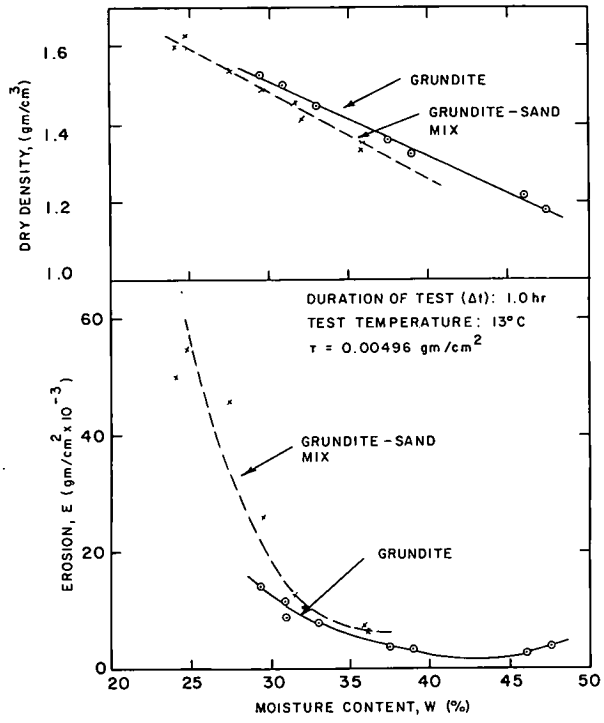

Mitchell et al. (10) recently considered bonding mechanisms and strength of soils in terms of rate process theory, using steady-state creep data as a basis for their hypotheses. The equation for creep rate is given in the form

$$\dot{\epsilon} = \chi \frac{kT}{h} \exp\left(-\frac{\Delta F}{RT}\right) \exp\left(\frac{\lambda \tau}{2SkT}\right) \tag{3}$$

where

$\dot{\epsilon}$ = creep strain rate,
τ = shear stress causing creep,
k = Boltzman's constant = 1.38×10^{-16} erg/deg K,
h = Planck's constant = 6.624×10^{-27} erg/sec,
T = absolute temperature, deg K,
R = universal gas constant = 1.98 cal/deg K,
ΔF = free energy of activation, cal/mole,
χ = a function that depends on the number of flow units in the direction of deformation and the average component of displacement in the same direction due to a single surmounting of the energy barrier,
λ = separation distance between successive equilibrium positions, and
S = number of flow units per unit area.

If the mechanism of erosion is similar to that of creep, it follows that the expression for erosion rate should be of the form

$$\dot{E} = \beta_E \exp(\alpha \tau_H) \tag{4}$$

where

$\beta_E = \sim T \exp\left(-\frac{\Delta F}{RT}\right)$ and

$\alpha = \frac{\lambda}{2SkT}$.

The exponential dependence of erosion rate on the hydraulic shear stress predicted by Eq. 4 can be seen from Figures 6 and 7.

From Eq. 4,

$$\frac{\partial \ln\left(\frac{E}{T}\right)}{\partial\left(\frac{1}{T}\right)} = -\frac{1}{R}\left(\Delta F - \frac{\lambda N \tau_H}{2S}\right) \tag{5}$$

where $N = \frac{R}{k}$ = Avogadro's number. Figures 10 and 11 show that the form of Eq. 5 correctly describes the effect of temperatures on the steady-state erosion rate.

The values of the rate process parameters have been computed from the data shown in Figures 6, 7, 10, and 11 and are given in Table 4. These values may be compared with those obtained by Mitchell et al. (10) to determine whether the rate process hypotheses developed from creep studies are applicable to erosion.

The number of bonds per unit area S computed from the erosion data is of the order of 5×10^5, which is approximately five orders of magnitude smaller than typical values reported for creep (10). However, Mitchell et al. (10) have also shown that the number of bonds is inversely proportional to compressive strength (or shear strength, τ_{max} in gm/cm^2); e.g., for remolded illite,

$$S \simeq (8 \times 10^7)\, \tau_{max} \tag{6}$$

The erosion tests indicated that, when the hydraulic tractive stress exceeded the critical value, significant shear failures were occurring, causing large clusters of soil to be removed from the clay lining. If the critical hydraulic tractive stress is interpreted as the shear strength of the soil at the exposed face of the lining, then, according to

Figure 10. Erosion rate as a function of absolute temperature for kaolinite.

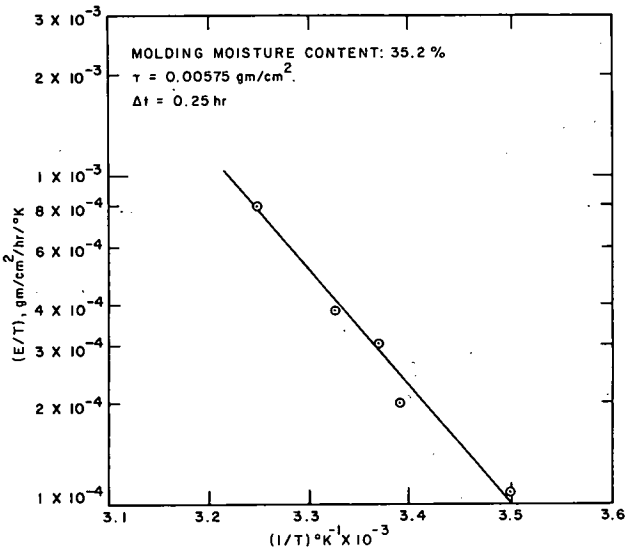

Figure 11. Erosion rate as a function of absolute temperature for grundite.

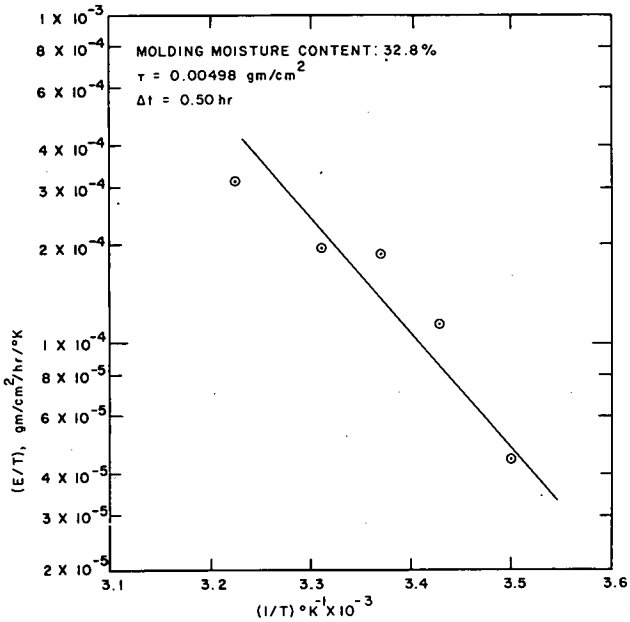

Table 4. Values of rate process parameters for kaolinite and grundite.

Soil Type	α (cm^2/gm)	β_ϵ ($gm/cm^2/hr$)	S (cm^{-2})	$\Delta F - \frac{\lambda N \tau_K}{2S}$ (cal/mole)
Kaolinite	200	5.8×10^{-3}	5.75×10^5	16,300
Grundite	120	8.1×10^{-4}	3.45×10^5	15,400

Eq. 6, S should be of the order of 10^5. Interpreted in this light, the apparently small number of bonds per unit area and the correspondingly high value of α are consistent with the concept of bonding proposed by Mitchell et al.

The experimental activation $\left(\Delta F - \frac{\lambda N \tau_H}{2S}\right)$ was computed from Eq. 6 and the data are shown in Figures 10 and 11. The values obtained for erosion are substantially lower than those reported for creep (10). As discussed previously, part of the discrepancy may be attributed to the fact that the accuracy of temperature control and measurement in this study were relatively crude for the calculation of activation energy. Therefore, it is quite possible that the actual values of activation energy should be higher than those calculated. However, it should also be noted that, by the very nature of the erosion process, data cannot be obtained until failure conditions are imminent at the surface of the clay lining. Hence, the experimental activation energy computed from the erosion tests pertains to conditions very near failure. Mitchell et al. (9) have shown that the experimental activation energy tends to decrease as failure is approached. Moreover, any contribution to the activation energy due to restraint of deformation caused by mechanical interaction between neighboring particles would be almost totally lacking in erosion from a free surface, whereas such effects could be significant in a typical creep test where the planes of deformation pass through the body of the specimen.

CONCLUSIONS

1. Erosion rates are highly dependent on soil composition. Both clay content and clay type are important variables.
2. Other important variables of soil erodibility appear to be surface roughness, flow rate, i.e., hydraulic tractive stress, and duration of flow.
3. There is a sharp point of demarcation at which the steady-state erosion rate rapidly increases with increasing hydraulic tractive stress. This point provides a convenient working definition for critical tractive stress.
4. In saturated soils, increased density does not necessarily increase resistance to erosion. Other factors related to placement conditions such as surface roughness may overshadow the effects of increased density.
5. Although more than one interpretation is possible, it is postulated that erosion of saturated cohesive soils is basically a shearing process that can be explained in terms of the rate process theory. By use of this approach, the values of the rate process parameters (activation energy and number of bonds) are consistent with those obtained for steady-state creep.

REFERENCES

1. Berghager, D., and Ladd, C. C. Erosion of Cohesive Soils. M.I.T., Dept. of Civil Eng., Res. Rept. R64-1, Jan. 1964.
2. Dunn, I. S. Tractive Resistance of Cohesive Channels. Jour. Soil Mech. and Found. Div., Proc. ASCE, Vol. 85, No. SM3, Proc. Paper 2062, June 1959, pp. 1-24.
3. Flaxman, E. M. Channel Stability in Undisturbed Cohesive Soils. Jour. Hydraulics Div., Proc. ASCE, Vol. 89, No. HY2, Proc. Paper 3462, March 1963, pp. 87-96.
4. Grissinger, E. H. Resistance of Selected Clay Systems to Erosion by Water. Water Resources Research, Vol. 2, No. 1, 1966, pp. 131-138.
5. Kennedy, R. B. The Prevention of Silting in Irrigation Canals. Proc., Institution of Civil Engineering, London, Vol. 119, 1895, pp. 281-290.
6. Lane, E. W. Design of Stable Channels. Trans. ASCE, Vol. 120, 1944, pp. 1234-1260.
7. Masch, F. D., Jr. Abstracted Bibliography on Erosion of Cohesive Materials. Jour. Hydraulics Div., Proc. ASCE, Vol. 92, No. HY2, Proc. Paper 4746, March 1966, pp. 243-289.

8. Masch, F. D., Jr. Erosion of Cohesive Sediments. Jour. Hydraulics Div., Proc. ASCE, Vol. 94, No. HY4, Proc. Paper 6044, July 1968.

9. Mitchell, J. K., Campanella, R. G., and Singh, A. Soil Creep as a Rate Process. Jour. Soil Mech. and Found. Div., Proc. ASCE, Vol. 94, No. SM1, Proc. Paper 5751, Jan. 1968, pp. 231-253.

10. Mitchell, J. K., Singh, A., and Campanella, R. G. Bonding, Effective Stresses, and Strength of Soils. Jour. Soil Mech. and Found. Div., Proc. ASCE, Vol. 95, No. SM5, Proc. Paper 6786, Sept. 1969, pp. 1219-1246.

11. Moody, L. F. Friction Factor for Pipe Flow. Trans. ASME, Vol. 66, 1944, pp. 671-684.

12. Moore, W. L., and Masch, F. D., Jr. Experiments on the Scour Resistance of Cohesive Sediments. Jour. Geophysical Research, Vol. 67, No. 4, April 1962, pp. 1437-1499.

13. Partheniades, E. Erosion and Deposition of Cohesive Soils. Jour. Hydraulics Div., Proc. ASCE, Vol. 91, No. HY1, Proc. Paper 4204, Jan. 1965, pp. 105-138.

14. Partheniades, E. Results of Recent Investigations on Erosion and Deposition of Cohesive Sediments. Sedimentation (Symposium to Honor Professor Hans A. Einstein, edited by Hsieh Wen Shen) Colorado State Univ., Fort Collins, 1972, pp. 20-1-20-39.

15. Partheniades, E., and Paaswell, R. E. Erosion of Cohesive Soils and Channel Stabilization, Part I: State of Knowledge. Dept. of Civil Eng., State University of New York, Buffalo, Civil Engineering Rept. 19, Oct. 1968.

16. Partheniades, E., and Paaswell, R. E. Erodibility of Channels With Cohesive Boundary. Jour. Hydraulics Div., Proc. ASCE, Vol. 96, No. HY3, March 1970, pp. 755-771.

17. Rowlison, D. L., and Martin, G. L. Rational Model Describing Slope Erosion. ASCE Annual and Environmental Meeting, Chicago, Preprint 1049, Oct. 1969.

18. Smerdon, E. T., and Beasley, R. P. The Tractive Force Theory Applied to Stability of Open Channels in Cohesive Soils. Univ. of Missouri, Res. Bull. 715, Agricultural Exp. Station, Oct. 1959.

19. Streeter, V. L. Fluid Mechanics. McGraw-Hill, New York, 1966.